Review Article

Multi-modal CT scanning in the evaluation of cerebrovascular disease patients

Luca Saba[1], Michele Anzidei[2], Mario Piga[1], Federica Ciolina[2], Lorenzo Mannelli[3], Carlo Catalano[2], Jasjit S. Suri[4,5], Eytan Raz[6,7]

[1]Department of Radiology, Azienda Ospedaliero Universitaria (A.O.U.), di Cagliari – Polo di Monserrato s.s. 554 Monserrato (Cagliari) 09045, Italy; [2]Departments of Radiological Sciences, University of Rome La Sapienza, Viale Regina Elena 324, 00161 (Rome), Italy; [3]Department of Radiology, University of Washington, Seattle, Washington, USA; [4]Fellow AIMBE, CTO, AtheroPoint LLC, Roseville, CA, USA; [5]Department of Biomedical Engineering, Idaho State University (Aff.), ID, USA; [6]Department of Radiology, New York University School of Medicine, New York, USA; [7]Department of Neurology and Psychiatry, Sapienza University of Rome, Viale dell' Università, 30, 00185 Rome, Italy

Correspondence to: Luca Saba, MD. Department of Radiology, Azienda Ospedaliero Universitaria (A.O.U.), di Cagliari – Polo di Monserrato s.s. 554 Monserrato (Cagliari) 09045, Italy. Email: lucasaba@tiscali.it.

Abstract: Ischemic stroke currently represents one of the leading causes of severe disability and mortality in the Western World. Until now, angiography was the most used imaging technique for the detection of the extra-cranial and intracranial vessel pathology. Currently, however, non-invasive imaging tool like ultrasound (US), magnetic resonance (MR) and computed tomography (CT) have proven capable of offering a detailed analysis of the vascular system. CT in particular represents an advanced system to explore the pathology of carotid arteries and intracranial vessels and also offers tools like CT perfusion (CTP) that provides valuable information of the brain's vascular physiology by increasing the stroke diagnostic. In this review, our purpose is to discuss stroke risk prediction and detection using CT.

Keywords: Computed tomography (CT); CT-angiography (CTA); CT perfusion (CTP); stroke; carotid artery; vulnerable plaque

Submitted Feb 17, 2014. Accepted for publication May 07, 2014.
doi: 10.3978/j.issn.2223-3652.2014.06.05
View this article at: http://dx.doi.org/10.3978/j.issn.2223-3652.2014.06.05

Introduction

Ischemic stroke currently represents one of the leading causes of severe disability and mortality in the western world and its early detection is extremely important (1,2). Several investigations have explored the risk factors for the development of ischemic events by confirming that the atherosclerotic disease of the carotid artery represents an important cause of the strokes (3,4).

Researchers have thus focused their attention on the diagnosis of the carotid artery pathology and on the detection of those markers that are associated with plaque vulnerability such as plaque composition, intra-plaque hemorrhage (IPH), fibrous cap rupture and plaque's ulcerations (5-10).

In the past years digital angiography (DA) was the imaging technique most used for the detection of the carotid artery pathology. However, a fundamental limit of DA is that it is a pure luminal methodology that offers information regarding only the lumen of the vessel but no information about the carotid wall and the plaque. Ultrasound (US), magnetic resonance (MR) and computed tomography (CT) have emerged as non-invasive imaging tools. These three techniques offer a detailed overview of the lumen of the vessel and the plaque and have completely come to substitute for the DA (11-15).

In particular, CT has tremendously evolved due to the software and hardware evolution by allowing for the acquisition of isotropic analysis with a spatial resolution of 0.4 mm (16-18). Several authors consider CT the best imaging modality for quantification of carotid artery stenosis and for the detection of some elements of plaque's

Table 1 CTA of supra-aortic vessels technical parameters

Items	Parameter
Intravenous contrast	40 to 60 mL (from 320 to 400 mgI)
Flow rate	4 to 6 mL/sec
Timing of image acquisition	Bolus tracking : 120 HU in the aortic arc
Scan distance	Aortic arch through the circle of Willis
mAs	120 to 150
kVp	120
Collimation	64×0.6
Slice thickness	0.75 mm
Interscan spacing	0.5 mm

CTA, CT-angiography.

Table 2 CTA of brain technical parameters

Items	Parameters
Intravenous contrast	30 to 40 mL (from 320 to 400 mgI)
Flow rate	4 to 6 mL/sec
Timing of image acquisition	Bolus tracking: 120 HU in the carotid
Scan distance	base of skull to vertex*
mAs	250 to 450
kVp	120
Collimation	64×0.6
Slice thickness	0.75 mm
Interscan spacing	0.5 mm

*, according to the vendor; CTA, CT-angiography.

vulnerability (such as ulcers). The main limitation of the CT study is the radiation dose [usually it ranges from 5 to 7 milli-Sievert (mSv)] delivered to the patients even if some methods can be used to reduce the radiation dose and multi-spectral scanner can perform a CTA of carotid arteries with 2 mSv (19).

In those patients with suspected ischemic stroke it is possible to perform CT perfusion (CTP) that offers valuable information of the brain's vascular physiology by increasing the stroke diagnostic performance, thereby providing useful additional information. By analyzing the cerebral blood volume (CBV), the cerebral blood flow (CBF), and mean transit time (MTT), it is also possible to obtain information about the ischemic penumbra. In this review our purpose is to discuss stroke risk prediction and detection using CT.

CT protocol

CT-angiography (CTA). The acquisition protocol markedly varies according to the type of scanner available because the velocity of acquisition can be very different. In our Institution we perform un-enhanced and enhanced scans. A peripheral venous access with an 18 or 20 gauge needle is obtained and the power injector is loaded with nonionic iodinated contrast material. Usually the right antecubital vein is selected in order to avoid artifacts due to the fact that undiluted contrast material in the subclavian artery might obscure the origins of the great vessels. The amount of contrast material is usually 40-60 mL followed by a 25-mL saline bolus chaser and the injection rate should be >4 mL/sec. The acquisition should cover from the aortic arch to the circle of Willis and it can be performed in caudo-cranial or cranio-caudal directions. Patients are placed in the supine position and they are instructed not to breathe or swallow. For this type of exam the best method to deliver the contrast medium is bolus tracking. In bolus tracking, a designated vessel of interest is monitored in real-time with low-dose dynamic scanning and when the selected enhancement threshold (from 80 to 120 HU) is reach, the scan begins (*Table 1*).

The technical parameters can significantly change according to the different equipment. In order to obtain a good level of quality the slice thickness should be <1 mm. The use of the dose modulation can be useful to reduce the dose of radiation delivered to the patients but sometimes this approach reduces the signal-to-noise ratio. CTA is followed by the CTP, using an additional bolus of 30-40 mL of contrast material. Four adjacent 5-mm slices are analyzed on the 16 slice scanners or eight 5-mm slices on the 64-slice scanner and time density curves are then calculated for each pixel and analyzed using vendor-based software (*Table 2*).

Post processing is performed by the technologist at the scanner or in the 3D laboratory. Maximum intensity projection (MIP) images of the carotid bifurcations are obtained bilaterally in sagittal oblique planes and the origins of the great vessels and extracranial carotid arteries are obtained in the coronal plane.

Diagnostic flow chart and role of CTA

The selection of patients requiring surgical/interventional treatment for carotid atherosclerotic disease is based on the degree of stenosis and presence of symptoms (Flow-chart: *Figure 1*). However, risk of embolism is not only due

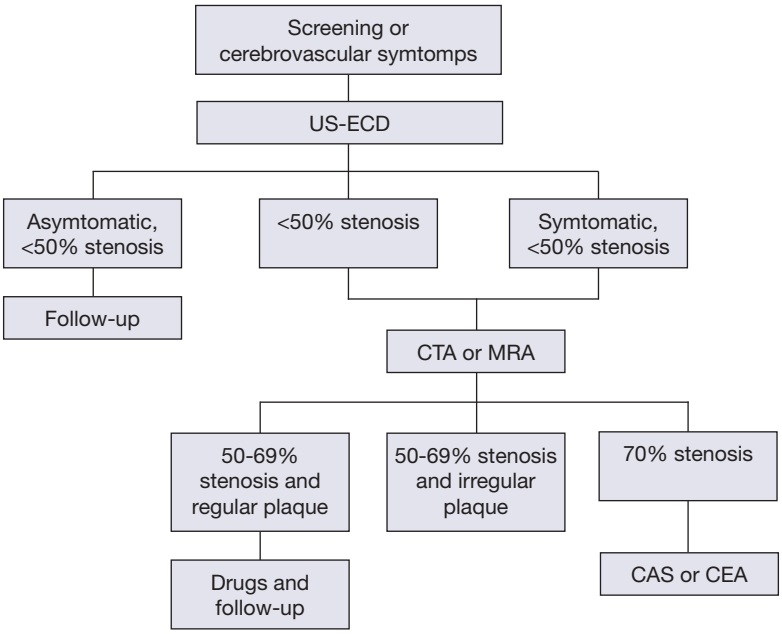

Figure 1 Imaging flow-chart. US, ultrasound; CTA, CT-angiography.

to presence, location and size of carotid plaque, but also to its composition. Therefore, the detection of vulnerable plaque and IPH is fundamental when choosing the correct therapeutical approach. US is an accurate and cost-effective non-invasive method for screening patients at risk for carotid atherosclerosis, used also in asymptomatic subjects scheduled for surgery such as coronary artery bypass graft, abdominal aortic aneurysm and lower limb ischemia (20). However, the role of CTA and MRA in the detection of carotid stenosis is increasing and in our Institution, CTA is currently considered the first choice examination in patients at high risk of cerebrovascular disease, reserving US for the evaluation of patients with a lower risk (21,22) or screening program. An important advantage of the CTA versus the US is the potentiality of CTA to explore the distal ICA and intra-cranial ICA and the consequent potential detection of tandem-lesions.

In patients with stenosis greater than 50% at US or less than 50% but symptomatic, CTA or MRA are suggested to confirm the diagnosis, to accurately determine the precise degree of stenosis and to plan appropriate treatment (i.e., detection of anatomical variants in vessel course, tandem lesions, intracranial atherosclerotic disease, etc.). No definitive conclusion exists as to which is the best technique regarding CTA and MRA (23-25) but since MRA is time-consuming, costly and not as easily available as CTA, the latter is the preferred diagnostic method in most centers. CTA allows for an optimal assessment of the morphology of the carotid plaque (the "inner lumen"), and differentiating between a smooth (*Figure 2*), irregular or ulcerated surface (*Figure 3*) (26). Plaque irregularities may be associated with increased risk for stroke/TIA or previous cerebrovascular adverse events. Ulcerated plaque is characterized by the presence of an intimal defect larger than 1,000 μm in width exposing the necrotic core of the plaque (27). Previous studies comparing CTA and US-ECD demonstrated that the diagnostic accuracy of CTA is significantly higher in the detection of ulceration (93% versus 37.5%) (9). Ulcerations of plaque can be classified into four types: plaque with an ulcer that comes out perpendicular to the lumen (type 1); plaque with a narrow neck showing a "mushroom shape" or no visible neck (type 2), plaque with an ulcer neck proximal and main part of the ulcer pointing distally (type 3) and plaque with an ulcer neck that is distal and points proximally (type 4). Irregular plaque's morphology and ulcerations are associated with IPH, lipid core, thin or ruptured fibrous cap and plaque instability (25).

CTA allows us to classify the type of plaque as fatty (soft plaque with density value <50 HU), mixed (density value between 50 and 119 HU) and calcified (density >120 HU) (28) placing a circular or elliptical region of interest (ROI) in the predominant area of the plaque

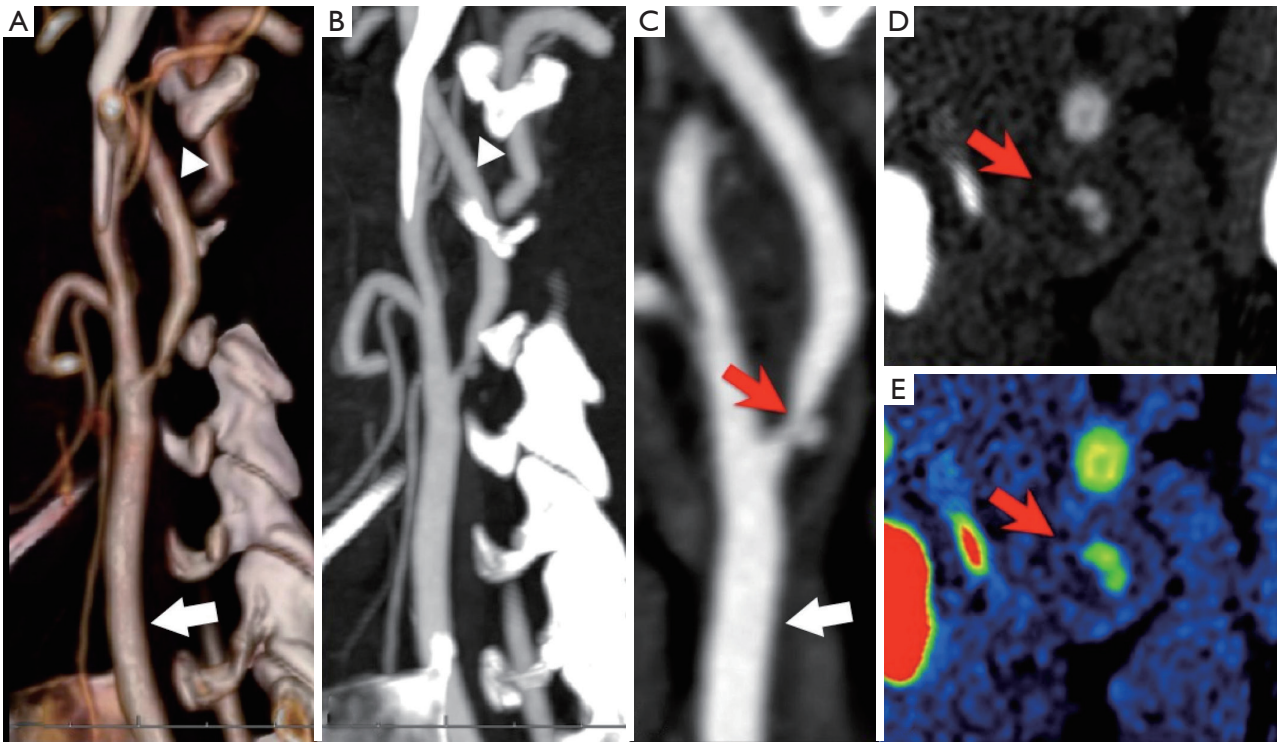

Figure 2 VR, MIP and multiplanar reconstruction show an ulcerated plaque of the carotid bifurcation (A-C) (red arrow). Axial images (D,E) show degree of stenosis, ulceration and composition of the plaque (low density). Common carotid artery is indicated by white arrows whereas internal carotid artery by white arrowheads. VP, volume rendered; MIP, maximum intensity projection.

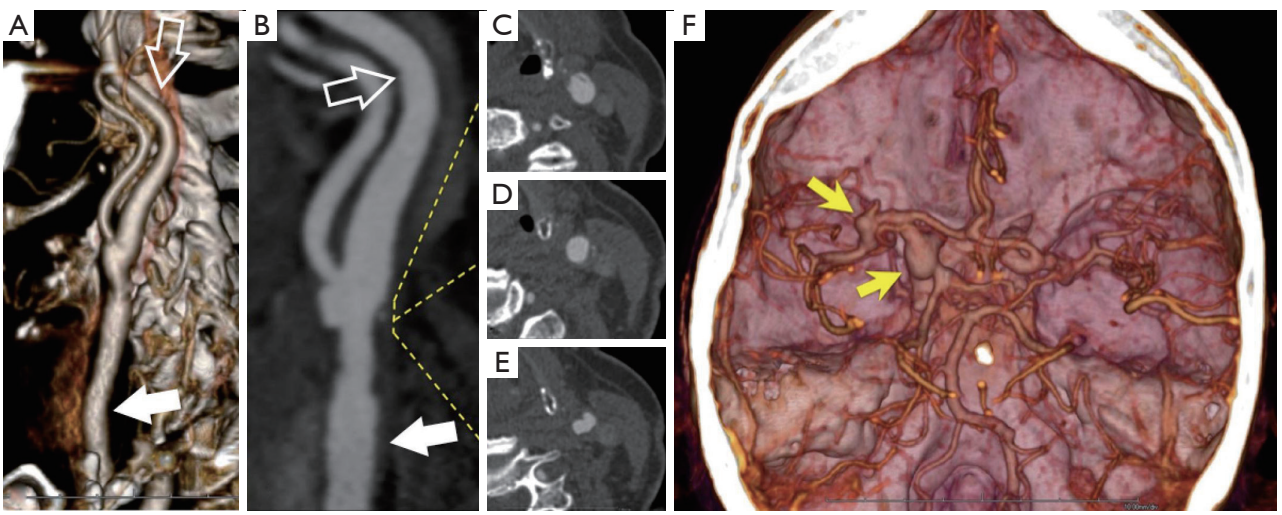

Figure 3 VR and MPR (A,B) show a non-significant stenosis caused by a smooth plaque with irregular and ulcerated surface (C-E). CTA incidentally detects the presence of two intracranial aneurysms (yellow arrow). Common carotid artery is indicated by white arrows whereas internal carotid artery by white open arrows. VR, volume rendered; MPR, maximum intensity projection; CTA, CT-angiography.

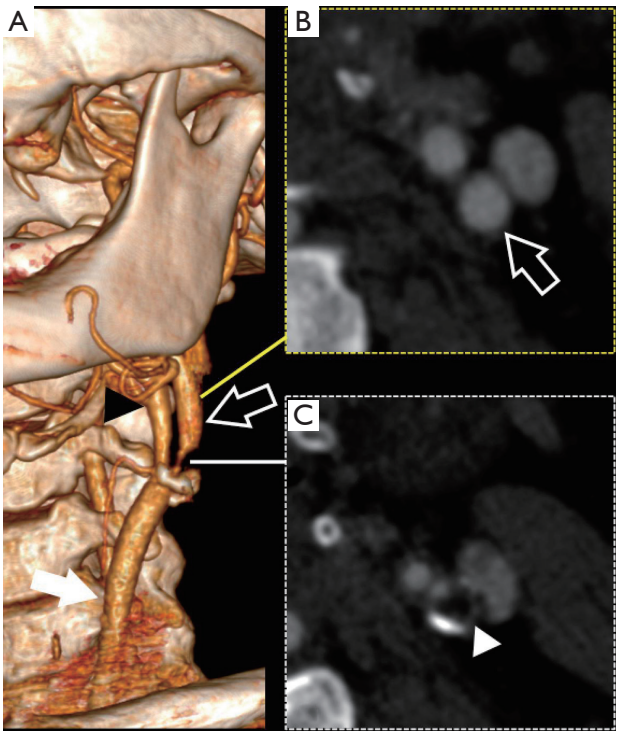

Figure 4 VR (A) and axial CTA images (B,C) of a 67-year-old patient with a severe stenosis in the left ICA. According to the NASCET the degree of stenosis is calculated with the ratio between the lumen diameter at the stenosis site (C) and lumen diameter of the distal, healthy internal carotid artery (B). VR, volume rendered; CTA, CT-angiography; NASCET, North American Symptomatic Carotid Endarterectomy Trial.

(9,10,25). An excellent inter-observer reproducibility has been reported in connection with this method and it has been demonstrated that HU values measured in the center of fibrous-rich regions and the lipid core are significantly different (29).

Another important risk factor that should be considered is the plaque volume: a moderate association between plaque volume and severity of luminal stenosis has been observed (30). Furthermore, recent studies have shown that CTA can measure carotid artery wall thickness (CAWT) and that there is a significant association between thicker CAWT (>1 mm) and stroke risk (P<0.0001).

Lastly, CTA may incidentally detect intracranial aneurysms: it has been reported an incidence of 4.1% intracranial aneurysm in presence of internal carotid artery stenosis (31), significantly higher compared to the general population, in which the prevalence is 2.3% (32); authors hypothesized that this relation may be explained by the fact that atherosclerotic diseases and intracranial aneurysms share common risk factors.

Quantification of degree of stenosis of carotid artery

The quantification of the degree of stenosis (*Figure 4*) is considered the leading parameter in selecting better treatment because of its correlation with risk of stroke. For this reason different multi-centric randomized trials have been performed to identify the cut-off values of stenosis degree that may benefit from carotid endarterectomy (CEA): North American Symptomatic Carotid Endarterectomy Trial (NASCET), the European Carotid Surgery Trial (ECST) and Asymptomatic Carotid Atherosclerosis Group (ACAS). The first two trials are the most frequently used: they evaluate the degree of stenosis as the percentage reduction in the linear diameter of the artery (measurements must be performed on a strictly perpendicular plane to the longitudinal axis of the vessel). The NASCET method measures the ratio between the diameter of the lumen at the point of maximum stenosis and the diameter of the lumen in the distal, healthy internal carotid artery, while the ECST method calculates the ratio between the diameter of the lumen at the stenosis site and the total carotid diameter (including the plaque). As a result, this measurement technique determines that ECST stenosis degree is larger compared to NASCET values (e.g., 83% ECST usually is a 70% NASCET). The difference in measurements has shown a wide variability (33).

The percentage-base methods are prone to inter-observer variability and errors, mostly due to incorrect detection of the arterial reference (the distal ICA for NASCET and the ICA lumen for ECST) and a new measurement method for CTA based on a direct mm measurement of carotid stenosis has been introduced by Bartlett *et al.* (34). This technique shows a linear relationship between the residual lumen of the internal carotid artery measured in mm on co-axial sections and NASCET stenosis, with a residual carotid diameter of 1.3 mm equivalent to 70% NASCET stenosis. This value has been proposed as the threshold for severe carotid stenosis, showing a sensitivity of 88% and a specificity of 92%.

Another important concept to consider is "near occlusion" condition (*Figure 5*) which indicates a presence of severe carotid bulb stenosis with homogeneous decrease of the caliber of the ICA distal to the bifurcation secondary

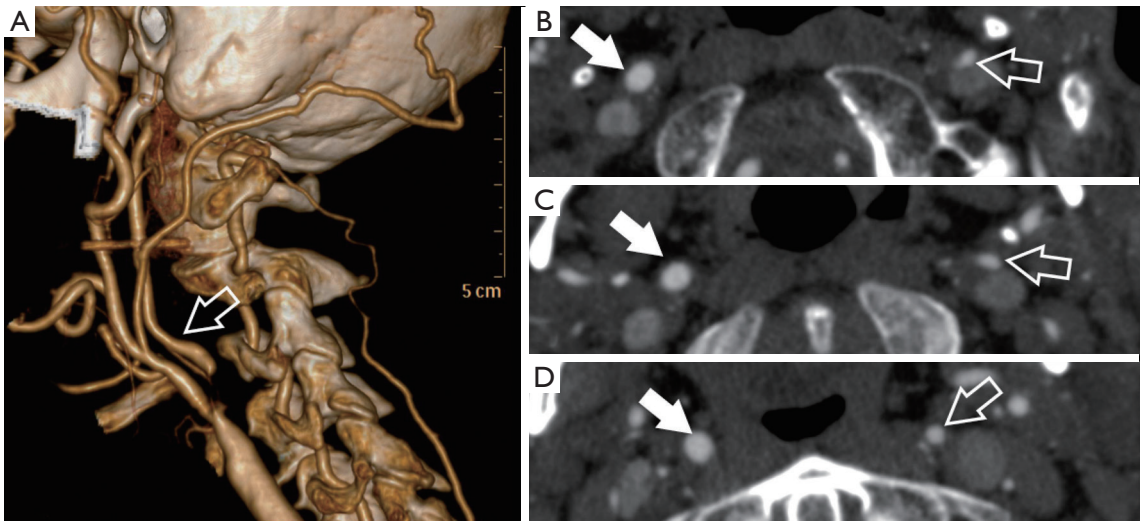

Figure 5 VR (A) and axial CTA images (B-D) of a 62-year-old patient with a near occlusion of the left ICA (white open arrow) that is markedly smaller compared to the right ICA (white arrow) in the different level (panel B at C3 level, panel C at C2 level and panel D at C1 level). VR, volume rendered; CTA, CT-angiography.

to flow reduction: detection of near-occlusion influences treatment planning since it has been demonstrated that this condition determines a lower risk of ipsilateral stroke and that CEA/revascularization is less effective (35). In these cases, the NASCET method fails in the determination of stenosis degree due to the lack of a distal healthy arterial reference. A near occlusion is defined as a stenosis of the ICA bulb with distal ICA caliber reduction compared to the contro-lateral internal carotid artery and the ipsilateral external carotid artery (ratio between caliber of distal ICA and ipsilateral ECA >1 is diagnostic for near occlusion) (20,34).

Carotid artery vulnerable plaque

As previously described, the degree of luminal stenosis (usually quantified by using the NASCET method) is considered the lead parameter for choosing the therapeutical approach (carotid endarterectomy—carotid artery PTA/stenting—best medical treatment); however, in the last few years, several researchers have demonstrated that the plaque structure may increase or reduce the risk of a patient developing an ischemic stroke. In particular, in 1989 Muller introduced the concept of "vulnerable plaque" identifying plaques (also with low degree of stenosis) susceptible to rupture and embolization (36). The vulnerable plaque is histologically characterized by a large eccentric necrotic core, covered by a thin fibrous cap (<65 μm), infiltrated by macrophages, inflammatory cells, spotty calcifications and vasa vasorum proliferation. Progression of atherosclerosis determines disintegration of the foam cells, loss of smooth muscle cell, while matrix metalloproteinases produced by inflammatory cells determines formation of a destabilizing lipid core which is fragile and prone to fibrous cap ruptures. Moreover, hypoxia in the inner layer of the vessel wall causes proliferation of fragile and immature microvessels that are sensitive to rupture with secondary bleeding (37).

Vulnerable plaque causes two thirds of acute events, with the remaining events caused by erosion of the intimal surface with thrombus formation (38). First angiographic and histopathological studies were conducted in coronary artery plaque, but similar findings were also found in carotid arteries by showing that cerebrovascular events can also be triggered in carotids with plaques that determine low grade stenosis (39-42).

Different invasive and noninvasive techniques were developed to image the morphology as well as the composition of the plaque. Authors found that the embolus detection during the trans-cranial Doppler may represent a very sensitive index of plaque instability (43). Currently the carotid artery plaques are imaged using mainly US, CTA or MRA. In particular, US is considered a first-line (screening exam) (11) even if recent papers have demonstrated that US can offer excellent detail of the carotid vulnerable plaque,

such as the presence and degree of neovascularization of the plaque (43). Another study (44) found that ultrasonic plaque echolucency and emboli signals predict stroke in asymptomatic carotid stenosis.

Today, CTA is considered an accurate method when assessing vessel wall, location, extension and morphology of the plaque as well as those features associated with plaque vulnerability such as presence of ulcerations, rupture of the fibrous cap, plaque remodeling and low plaque density (<30 HU) (9,10,41,45-47). Thanks to the potential of CT to characterize the tissues, according to the HU attenuation, a classification of the type of plaque (fatty, mixed or calcified) has been proposed. The first attempt to classify the plaques according to the attenuation was performed by Schroeder *et al*. in 2001 assessing coronary arteries (48) (fatty plaques <50 HU, mixed plaques between 50 and 120 HU, calcified plaques >120 HU). A few years later the Rotterdam group lead by van der Lugt performed a similar analysis on the carotid artery plaques (49,50) by determining thresholds for tissue classification in carotid arteries similar to the plaques in the coronary arteries (fatty plaques <60 HU, mixed plaques between 60 and 130 HU, calcified plaques >120 HU).

Several pieces of evidence suggest that fatty plaques with low attenuation values are associated with the vulnerability of the plaque even if clinical relationship still remains debated (51). Studies show that an increased risk of cerebrovascular events is expected (4,13). This is even more evident in recent studies that have demonstrated that the IPH in the plaque shows very low attenuation values (52,53).

Recent studies also pointed out the attention to the contrast enhancement that the carotid plaques may show after the administration of contrast material and its association with cerebrovascular events (54).

Other authors showed that the carotid plaque characteristics change and therefore those determinants of vulnerability might disappear after time. In particular van Gils *et al*. (55) found that in some cases carotid ulcers healed even if most of carotid ulcerations persist for a long time whereas usually plaque surface morphology remains unchanged. These findings allow for the hypothesis that carotid plaque morphology and characteristics may change between patients with acute stroke and patients with chronic cerebrovascular disease.

Moreover, CTA offers the possibility to directly see vulnerable plaques by using new iodinated contrast agent that selectively accumulates into macrophages (56). Automated software enables delineation of vessel walls, detection of plaque and attribution of a color to pixel with different attenuation value. In this way characterization of the plaque is possible. Despite the high accuracy, the method is affected by some limitations such as blooming artifacts in the presence of big calcification and radiation exposure (57).

The introduction of multi-energy CT scanners allows for further exploration of the carotid artery plaques by demonstrating which tissues have an increased or reduced attenuation according to the level of kiloelectron voltage applied (58,59). This approach helps to further characterize the tissue composition of the plaque by widening the CTA potentiality in the plaque assessment.

Evaluation of arterial intracranial circulation

Other than allowing for evaluation of the cervical arteries, CTA helps in defining possible intracranial arterial disease. CTA is a widely available and very accurate technique that, in the event of a stroke, allows determination of arterial occlusion and dissection and permits rapid assessment of vascular anatomy before treatment of acute stroke, giving information such as collateral circulation and intracranial atherosclerosis (60). In case of an intracranial artery occlusion, the interventional neuroradiologist will use the information provided from the CTA to predict the extent and location of the final infarction.

CTA has a high specificity and sensitivity for detecting occlusions as distal as the M2 segment of the middle cerebral artery (60,61). CTA is important for the detection of posterior circulation thrombosis, mainly for two reasons: the low sensitivity of unenhanced CT for detection of those infarctions and the fact that posterior fossa is not covered by the standard perfusion protocol (62). To evaluate the intracranial CTA, multiplanar MIP reformatting should be created. Additional views can be created in particular cases, such as a detail view, an MPR or a 3D volume rendering view (*Figure 6*). Unenhanced CT does not show the arterial occlusion, except in patients with a hyperdense arterial sign with high specificity but low sensitivity for an occluded cerebral artery, an often difficult to interpret sign (*Figure 7*) (63). The localization of the hyperdense arterial sign is considered a parameter that may predict the patient's outcome: when M1 (or even M2) segments are involved authors described a very poor outcome, whereas when M3-4 segment is involved usually the outcome is good (64-66). Regarding the evaluation of collateral vessels, it is notable that survival of brain parenchyma in the presence of an arterial occlusion depends on the above-mentioned leptomeningeal collateral

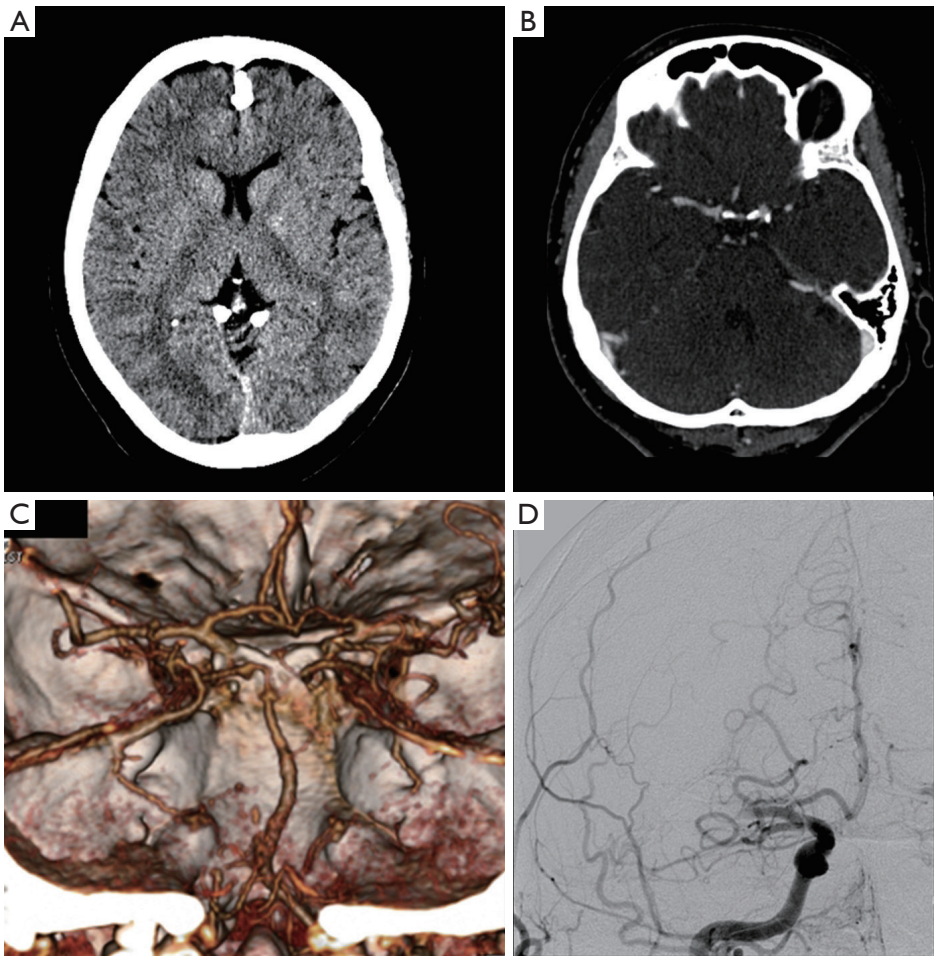

Figure 6 A 59-year-old female with acute onset of left-sided weakness and clinical suspicion for stroke. CT stroke series included a non-enhanced CT (A), which demonstrates minimal gray-white matter loss of differentiation and loss of the definition of the right basal ganglia. CTA (source image on B and VR on C demonstrates abrupt termination of the contrast column in the right middle cerebral artery distal M1 segment. This is confirmed on the subsequently performed DSA (D). CT, computed tomography; CTA, CT-angiography; VR, volume rendered.

pathways (67). Leptomeningeal collateral pathways are direct arteriolar anastomoses between pial branches which contribute to retrograde filling of pial arteries distal to an occlusion. Evaluation of leptomeningeal collaterals can be made using CTA (68). As logically expected, patients with better pial collaterals have a better prognosis (69). Leptomeningeal collaterals on CTA are also a reliable marker of good outcome in ischemic stroke. In a recently published paper the role of CTA in the evaluation of collateral circulation was explored: in 196 patients with complete occlusion of the intracranial internal carotid artery and/or the middle cerebral artery (M1 or M2 segments) The leptomeningeal collateral pattern was graded as a 3-category ordinal variable (less, equal, or greater than the unaffected contralateral hemisphere) and the authors found that presence of leptomeningeal collaterals (grade 3) was identified as independent predictors of a good outcome (OR, 1.93; 95% CI, 1.06-3.34; P=0.03) (70).

The whole brain analysis of the source images is very useful for a few reasons. Source images give direct information about flow of contrast into the tissues (71), providing a whole-brain perfusion map. Unlike CTP images, CTA source images cover the entire brain and are available immediately at completion of imaging, without requiring any form of postprocessing (72). CTA source images are more accurate than non-enhanced CT scans in

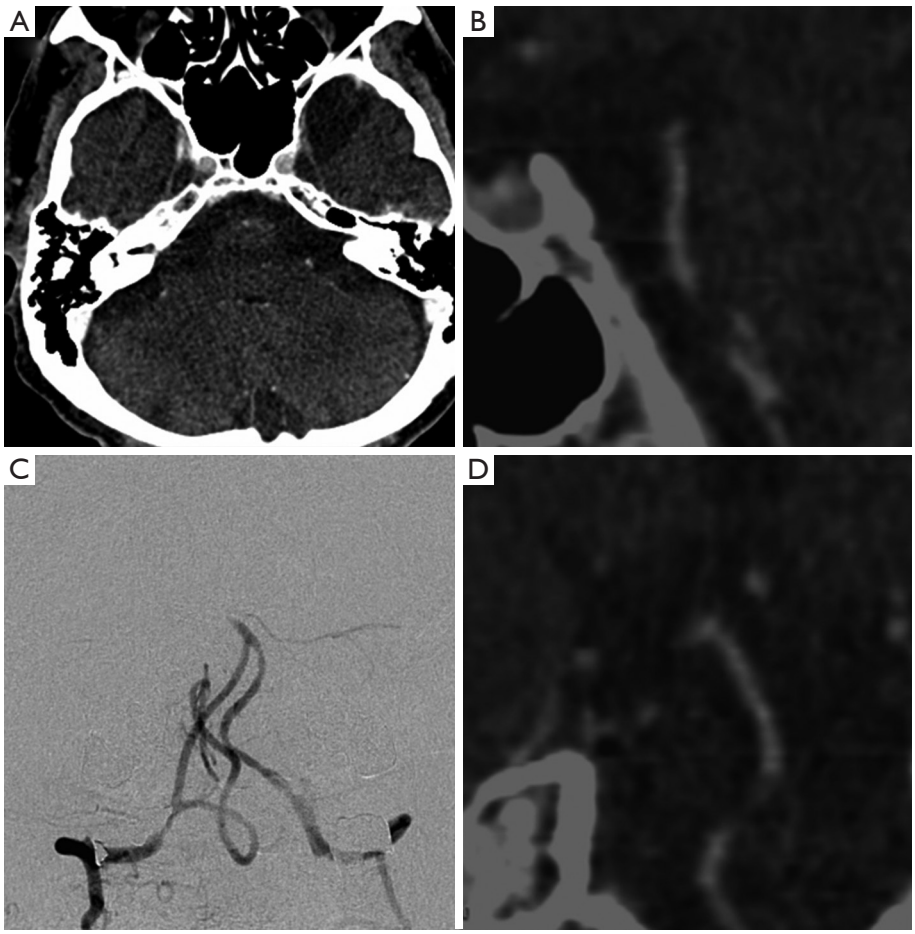

Figure 7 A 63-year-old male with acute onset of asymmetric quadriparesis, alteration in the level of consciousness and oculomotor abnormalities, suspicious for a basilar artery territory infarction. Unenhanced CT was negative. CTA (source image on A and detailed MPR on B and C) demonstrates a focal occlusion in the proximal basilar artery. This was confirmed on the subsequently performed DSA (D). CT, computed tomography; CTA, CT-angiography.

the prediction of final infarct volume, as measured by using ASPECTS score.

CT imaging of the vein

Cerebral sino-venous thrombosis (CSVT) is an uncommon disorder that involves the venous sinus and cerebral veins (73). The detection of this condition is important because the clinical presentation is usually nonspecific and when it progresses rapidly it can be lethal. The CT can help in detection and characterization of the CSVT and it is possible to identify findings in the un-enhanced phase as well as in the enhanced phase. In the un-enhanced phase it is possible to identify the "dense triangular sign" whereas after administration of contrast material the "cord sign" and the "empty delta sign" is a triangular defect determined by the enhanced dura surrounding the thrombus (*Figure 8*).

Previous investigations showed that after CSVT parenchymal changes can occur and a classification was suggested (73,74): stage I—no parenchymal change; stage II—brain swelling, sulci effacement and mass effect; stage III—reduction of the density as mild to moderate edema; stage IV—severe edema, with or without hemorrhage; and stage V—massive edema and/or hemorrhage.

According to previous studies, failure to diagnosis CSVT or underestimation of sinus involvement and venous infarcts by using CT were reported in up to 40% of patients (73,75). However, there are some conditions that can mimic venous sinus thrombosis in unenhanced CT. In particular, authors found that subarachnoid hemorrhage along the edges of the

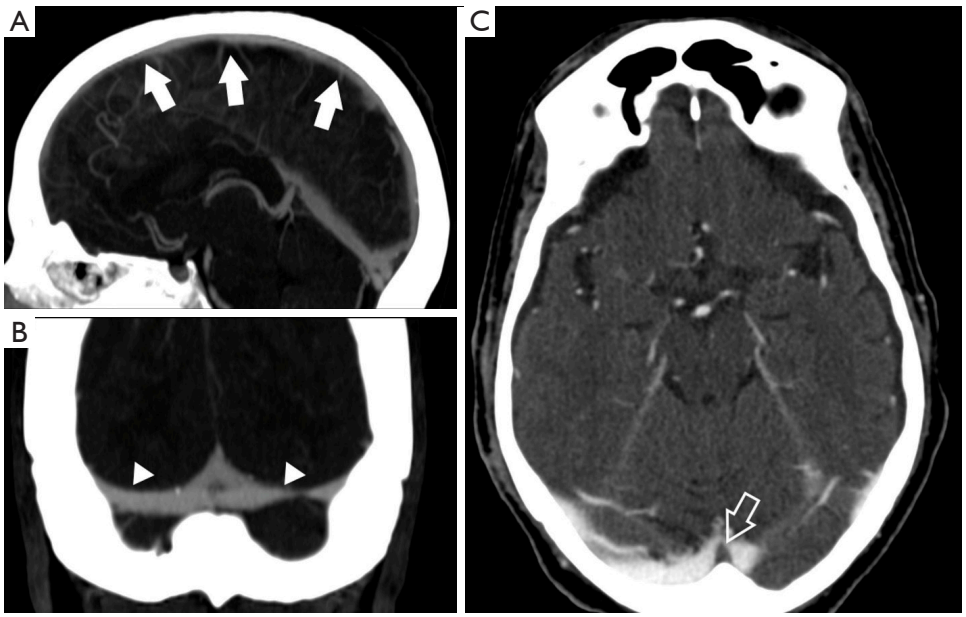

Figure 8 MIP (A,B) of a 37-year-old female patient with normal venous intra-cerebral system. The superior sagittal sinus is visible (white arrows) as well as the straight sinus (white arrowhead). In panel C the CTA axial image of a 42-year-old patient with headache that demonstrated the presence of thrombus at the confluence of sinuses (white open arrow). MIP, maximum intensity projection; CTA, CT-angiography.

tentorium cerebelli can be mistaken for CSTV (76).

Authors found that symmetry of venous sinuses identified by CT was correlated to an impaired cerebral reserve also in chronic conditions as atherosclerotic spontaneous occlusion of internal carotid artery (77). Moreover, the venous drainage also effects brain perfusion and collateral flow as indicated by Liebeskind (78).

CTP of the brain for stroke detection

Perfusion CT is usually performed after unenhanced CT and CTA. While these two exams demonstrate the vascular anatomy, CTP is a study suited for the evaluation of brain vascular physiology. The information provided by CTP may actually prolong the reperfusion time window giving similar information compared to those provided by an MRI (79). CTP increases the stroke diagnostic performance providing useful additional information to relatively inexperienced readers compared to the information given by stroke protocols which include only unenhanced CT and CTA (80). CTP involves a continuous cine CT imaging over around 45 seconds on a slab covering the same area of brain parenchyma during the administration of a bolus of contrast at high flow rate (81). CTP is hence obtained by monitoring the first pass of the contrast through the cerebral vasculature, evaluated using a model of linear relationship between contrast agent concentration and attenuation in Hounsfield Units (82). The following evaluation includes the visualization of different derived maps: CBV, CBF, MTT, and time to peak (TTP) (*Figure 9*). The parameters are related according to the following equation: CBF = CBV/MTT (*Figure 10*) (83). To obtain those maps, the contrast time-concentration curves are generated in an arterial ROI, in a venous ROI, and for each pixel with placement of ROIs in an input artery [usually the ACA or middle cerebral artery (MCA)] and an input vein, such as the torcular herophili. The software then generates color-coded CBF, CBV, and MTT maps (84).

The evaluation of acute stroke is the main indication for CTP, with which we can distinguishing infarcted non-vitalized tissue from the penumbra (*Figures 11*,*12*) (85), the penumbra being the tissue salvageable with thrombolytic agents, while infarcted non-vitalized tissue is irreversibly damaged with no benefit from reperfusion and at increased risk of hemorrhage after thrombolysis. Notably, this evaluation transcends an arbitrary clock time (86), possibly demonstrating that the reperfusion time window should be based on the single patient due to the highly variable

Figure 9 A 67-year-old male with a frontal lobe. The first video—CBF and CBV (Cerebral blood flow and cerebral blood volume), the second with the CBF and the third with the CBV demonstrate a left frontal cortical-subcortical area of decreased CBF and decreased CBV without mismatch are noted in the same location. All maps are color-coded red blue for low values and red for high values. CBF, cerebral blood flow; CBV, cerebral blood volume.

regional ischemic vulnerability. Ischemic core has a decrease in both CBF and CBV, whereas the penumbra demonstrates a reduction in CBF with a relatively maintained CBV. The CBV is maintained in the penumbra because the decreased perfusion pressure causes dilation of pre-capillary arterioles and engorgement of veins (87), while in the ischemic core, the reduction of CBF and CBV is related to the failure of autoregulation with consequent hypoperfusion. Tissue at risk of infarction will also have elevated MTT. Hence, patients with large CBV-MTT mismatch are the best candidates for reperfusion therapy, even after the first 3 hours after stroke onset (*Figure 13*) (88). After the stroke, postischemic hyperperfusion is another entity that can take advantage of CTP. Postischemic hyperperfusion represents the restoration of perfusion pressure close to normal values in the vascular territory previously affected by severe ischemia (89,90). Notably, areas of hyperperfusion within the brain parenchyma in the setting of stroke should

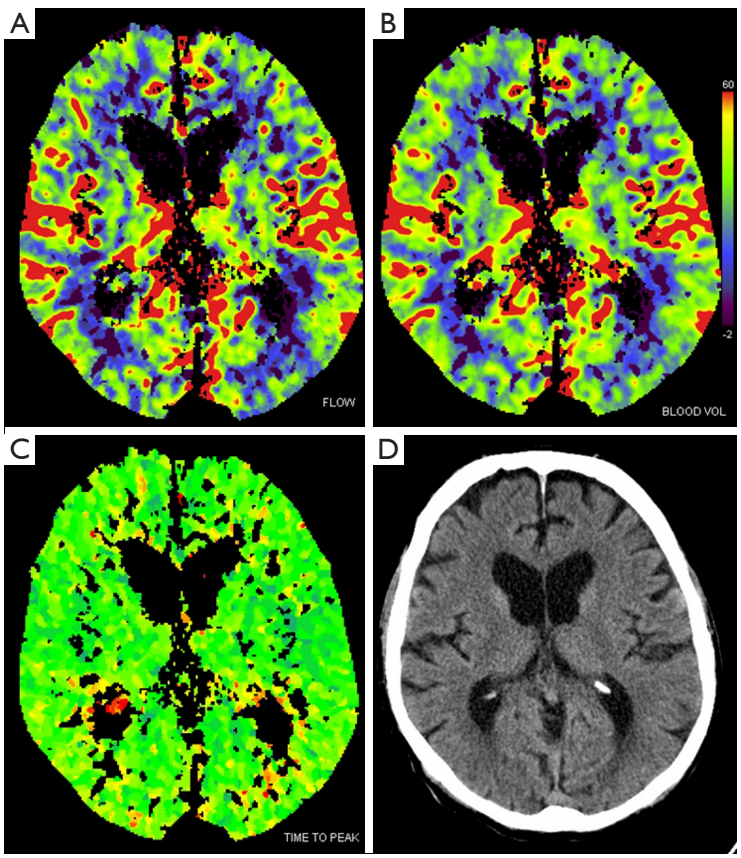

Figure 10 A healthy 42-year-old man. CT perfusion maps showing cerebral blood flow (A), cerebral blood volume (B), time to peak (C), demonstrates normal symmetric brain parenchyma perfusion. All maps are color-coded red blue for low values and red for high values. CT, computed tomography.

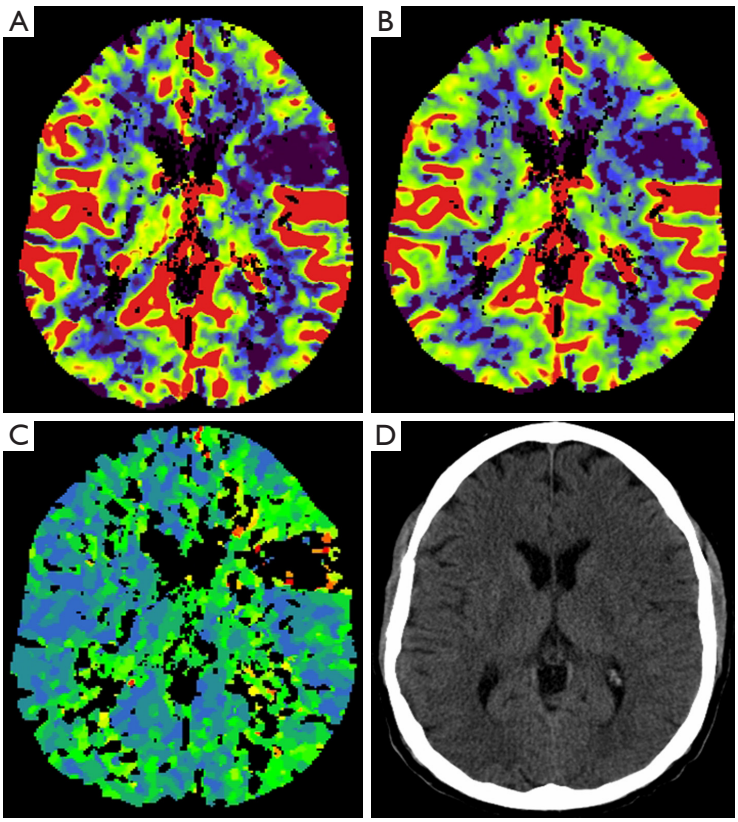

Figure 11 A 55-year-old male with acute onset of slurred speech, suspicious for a left frontal infarction. CTP maps showing CBF (A), CBV (B), TTP (C), demonstrates a left frontal cortical-subcortical area of decreased CBF and decreased CBV without mismatch are noted in the same location. There is, however, a very small mismatch between the TTP and the CBF and CBV maps. Notably, the unenhanced CT (D) performed right before the CTP was negative. CT, computed tomography; CBF, cerebral blood flow; CBV, cerebral blood volume; TTP, time to peak; CTP, CT perfusion.

not be abnormally interpreted as contralateral areas of hypoperfusion and acute infarction (91).

Clinical relevance of CTA-CTP

The clinical relevance of CTA and CTP has recently been demonstrated. Coutts *et al.* (92,93) have investigated in the prospective CATCH trial the predictive value of CTA in recurrent stroke in a population of 510 patients and they found that the early assessment of the intracranial and extracranial vasculature using CT/CTA predicts recurrent stroke and clinical outcome in patients with transient ischemic attack and minor stroke (hazard ratio, 4.0; 95% CI, 2.0-8.5). In patients with intracerebral haemorrhage (ICH), early haemorrhage expansion affects clinical outcome and investigators from the PREDICT study found that the CTA can predict the haematoma expansion (93,94).

The CTP value was underlined in the paper by Parsons *et al.* (95) where the authors used this technique to define the ischemic penumbra and the infarct core in order to select patients that underwent tenecteplase treatment.

CTA-CTP drawbacks

The main limitation of CTA is the delivered radiation dose (usually it ranges from 5 to 7 mSv). These values may represent a high level of delivered radiation, particularly in female patients of reproductive age, and the use of CTA in young-med-aged patients should be critically reviewed. However, it is important to underline that various methods can be used to reduce the radiation dose and that multi-spectral scanners can perform a CTA analysis in 2 mSv (19). The main

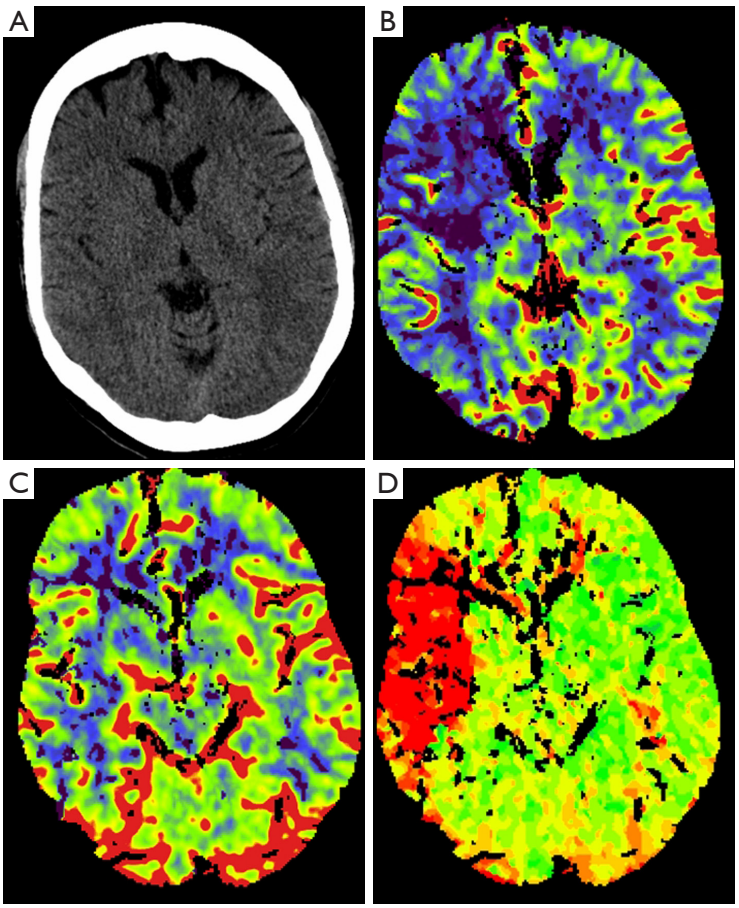

Figure 12 A 63-year-old female with acute onset of left-sided weakness, profound left neglect and right gaze preference. Unenhanced CT (A) demonstrates very mild symmetric density within the right middle cerebral artery territory. CTP maps showing CBF (B), CBV (C), MTT (D), demonstrates a right large area of decreased CBF (B) and a relative maintained CBV (C). There is elevated MTT (D), suggesting a large penumbra. CT, computed tomography; CTP, CT perfusion; CBF, cerebral blood flow; CBV, cerebral blood volume; TTP, time to peak; MTT, mean transit time.

drawback of the radiation is the increased stochastic risk of developing cancer (96).

Another potential limitation is the possible contrast toxicity because of the potential detrimental interaction of iodinated contrast with thrombolytic drugs (97,98).

CTP has some drawbacks that should be noted. First, as with CTP, the radiation dose presents a problem. In late 2009, excessive radiation dose during CTP was covered by the media after learning about 206 patients exposed to excess radiation at Cedars-Sinai Medical Center in Los Angeles over an 18-month period. This was followed by reports of excess radiation in >50 additional patients from other states, prompting an investigation by the FDA which issued an initial safety notification (99). The protocols that led to safety concerns in some US sites deviated from normal use and certainly from use in stroke, however it is important to underline that the typical exposure from a single CTP examination is around 2-10 mSv, similar to head CT alone and much lower than that from a full length CTA. Notably, the newest scanners have optimized protocols, allowing for stroke imaging with CTP to be done with an acceptable amount of radiation (100). In the CTA/CTP analysis it is mandatory to adopt some dose reduction strategies. The first one is to fix the tube current by taking patient size into account when selecting the parameters that affect radiation dose (in particular the mAs) (101,102). The second option is to use the tube-current (mA) modulation because it is demonstrated that extremely large variations

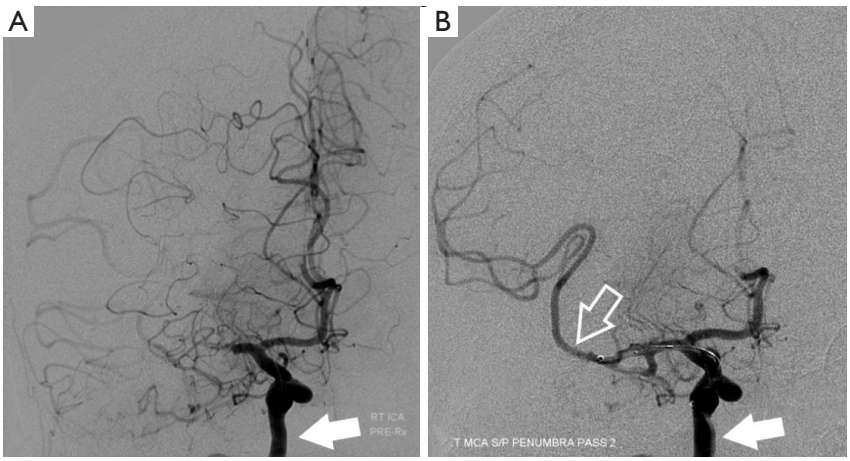

Figure 13 A 63-year-old female with acute stroke, same patient of *Figure 8*. Cerebral angiogram (A) demonstrates a fully occluding thromboembolus within the proximal M1 segment of the right middle cerebral artery, with evidence of some collateral to superior convexity and temporal regions, the former via anterior cerebral artery leptomeningeal branches. Same view demonstrates recanalization of multiple middle cerebral artery branches (B) after intra-arterial thrombolysis and thrombectomy performed with administration of t-PA and penumbra device reperfusion and direct mechanical thrombectomy. Internal carotid artery is indicated by white arrows whereas middle cerebral artery by white open arrow.

in patient absorption occur according to the anatomic area explored and this parameter is not considered when using a fixed tube current. Therefore, information acquired through body parts having less attenuation can be obtained with substantially less radiation. More advanced modalities for obtaining dose reduction are the automatic exposure control (AEC) and the iterative reconstruction. With the AEC, the CT systems adjusts the X-ray tube current in real time in response to variations in X-ray intensity at the detectors; with the iterative reconstruction the dose reduction is obtained through a significant reduction in the number of required projection views (and therefore of the necessary X-rays), while still producing acceptable image quality (101).

A second drawback is the volume-of-interest in TCP because it usually only covers a portion of the brain, which varies according to the manufacturing characteristics of the CT scanner.

Conclusions

In this review we aimed to discuss stroke risk prediction and detection using CT Angiography. Rapid improvement in the hardware and software has resulted in CT scanners that can detect and characterize the stroke and its cause (atherosclerotic pathology of supra-aortic vessels) with an exquisite level of detail. CTP offers valuable information about the brain vascular physiology thus increasing the stroke diagnostic performance.

Acknowledgements

The authors are deeply grated to Mrs Lia Tsarnas for her precious help in revising the manuscript.
Disclosure: The authors declare no conflict of interest.

References

1. Kim AS, Johnston SC. Global variation in the relative burden of stroke and ischemic heart disease. Circulation 2011;124:314-23.
2. Saposnik G, Kapral MK, Liu Y, et al. IScore: a risk score to predict death early after hospitalization for an acute ischemic stroke. Circulation 2011;123:739-49.
3. Saba L, Sanfilippo R, Pirisi R, et al. Multidetector-row CT angiography in the study of atherosclerotic carotid arteries. Neuroradiology 2007;49:623-37.
4. Saba L, Montisci R, Sanfilippo R, et al. Multidetector row CT of the brain and carotid artery: a correlative analysis. Clin Radiol 2009;64:767-78.
5. Saba L, Potters F, van der Lugt A, et al. Imaging of the fibrous cap in atherosclerotic carotid plaque. Cardiovasc

Intervent Radiol 2010;33:681-9.
6. Singh N, Moody AR, Gladstone DJ, et al. Moderate carotid artery stenosis: MR imaging-depicted intraplaque hemorrhage predicts risk of cerebrovascular ischemic events in asymptomatic men. Radiology 2009;252:502-8.
7. Wasserman BA. Advanced contrast-enhanced MRI for looking beyond the lumen to predict stroke: building a risk profile for carotid plaque. Stroke 2010;41:S12-6.
8. Yuan C, Mitsumori LM, Ferguson MS, et al. In vivo accuracy of multispectral magnetic resonance imaging for identifying lipid-rich necrotic cores and intraplaque hemorrhage in advanced human carotid plaques. Circulation 2001;104:2051-6.
9. Saba L, Caddeo G, Sanfilippo R, et al. CT and ultrasound in the study of ulcerated carotid plaque compared with surgical results: potentialities and advantages of multidetector row CT angiography. AJNR Am J Neuroradiol 2007;28:1061-6.
10. Saba L, Caddeo G, Sanfilippo R, et al. Efficacy and sensitivity of axial scans and different reconstruction methods in the study of the ulcerated carotid plaque using multidetector-row CT angiography: comparison with surgical results. AJNR Am J Neuroradiol 2007;28:716-23.
11. Saba L, Anzidei M, Sanfilippo R, et al. Imaging of the carotid artery. Atherosclerosis 2012;220:294-309.
12. U-King-Im JM, Fox AJ, Aviv RI, et al. Characterization of carotid plaque hemorrhage: a CT angiography and MR intraplaque hemorrhage study. Stroke 2010;41:1623-9.
13. Saba L, Sanfilippo R, Sannia S, et al. Association between carotid artery plaque volume, composition, and ulceration: a retrospective assessment with MDCT. AJR Am J Roentgenol 2012;199:151-6.
14. Saba L, Sanfilippo R, Montisci R, et al. Carotid artery stenosis at MSCT: is there a threshold in millimeters that determines clinical significance? Cardiovasc Intervent Radiol 2012;35:49-58.
15. Saba L, Mallarini G. Fissured fibrous cap of vulnerable carotid plaques and symptomaticity: are they correlated? Preliminary results by using multi-detector-row CT angiography. Cerebrovasc Dis 2009;27:322-7.
16. Saba L, Sanfilippo R, Anzidei M, et al. Stenosis Asymmetry Index (SAI) between symptomatic and asymptomatic patients in the analysis of carotid arteries. A study using CT angiography. Eur J Radiol 2012;81:77-82.
17. Saba L, Sanfilippo R, Montisci R, et al. Associations between carotid artery wall thickness and cardiovascular risk factors using multidetector CT. AJNR Am J Neuroradiol 2010;31:1758-63.
18. Saba L, Sanfilippo R, Pascalis L, et al. Carotid artery abnormalities and leukoaraiosis in elderly patients: evaluation with MDCT. AJR Am J Roentgenol 2009;192:W63-70.
19. Saba L, Mallarini G. Differences between MIP and MPR techniques in the carotid artery stenosis degree measurement. Evaluation using multi-detector-row CT angiograph. Minerva Cardioangiol 2008;56:21-7.
20. Wardlaw JM, Chappell FM, Stevenson M, et al. Accurate, practical and cost-effective assessment of carotid stenosis in the UK. Health Technol Assess 2006;10:iii-iv, ix-x, 1-182.
21. Héman LM, Jongen LM, van der Worp HB, et al. Incidental intracranial aneurysms in patients with internal carotid artery stenosis: a CT angiography study and a metaanalysis. Stroke 2009;40:1341-6.
22. Jaff MR, Goldmakher GV, Lev MH, et al. Imaging of the carotid arteries: the role of duplex ultrasonography, magnetic resonance arteriography, and computerized tomographic arteriography. Vasc Med 2008;13:281-92.
23. Wardlaw JM, Chappell FM, Best JJ, et al. Non-invasive imaging compared with intra-arterial angiography in the diagnosis of symptomatic carotid stenosis: a meta-analysis. Lancet 2006;367:1503-12.
24. Chappell FM, Wardlaw JM, Young GR, et al. Carotid artery stenosis: accuracy of noninvasive tests--individual patient data meta-analysis. Radiology 2009;251:493-502.
25. Noguchi T, Kawasaki T, Tanaka A, et al. High-intensity signals in coronary plaques on noncontrast T1-weighted magnetic resonance imaging as a novel determinant of coronary events. J Am Coll Cardiol 2014;63:989-99.
26. de Weert TT, Cretier S, Groen HC, et al. Atherosclerotic plaque surface morphology in the carotid bifurcation assessed with multidetector computed tomography angiography. Stroke 2009;40:1334-40.
27. Sitzer M, Müller W, Siebler M, et al. Plaque ulceration and lumen thrombus are the main sources of cerebral microemboli in high-grade internal carotid artery stenosis. Stroke 1995;26:1231-3.
28. Endarterectomy for asymptomatic carotid artery stenosis. Executive Committee for the Asymptomatic Carotid Atherosclerosis Study. JAMA 1995;273:1421-8.
29. de Weert TT, Ouhlous M, Meijering E, et al. In vivo characterization and quantification of atherosclerotic carotid plaque components with multidetector computed tomography and histopathological correlation. Arterioscler Thromb Vasc Biol 2006;26:2366-72.
30. Ouhlous M, Flach HZ, de Weert TT, et al. Carotid plaque

composition and cerebral infarction: MR imaging study. AJNR Am J Neuroradiol 2005;26:1044-9.
31. Héman LM, Jongen LM, van der Worp HB, et al. Incidental intracranial aneurysms in patients with internal carotid artery stenosis: a CT angiography study and a metaanalysis. Stroke 2009;40:1341-6.
32. Rinkel GJ, Djibuti M, Algra A, et al. Prevalence and risk of rupture of intracranial aneurysms: a systematic review. Stroke 1998;29:251-6.
33. Saba L, Mallarini G. A comparison between NASCET and ECST methods in the study of carotids: evaluation using Multi-Detector-Row CT angiography. Eur J Radiol 2010;76:42-7.
34. Bartlett ES, Walters TD, Symons SP, et al. Quantification of carotid stenosis on CT angiography. AJNR Am J Neuroradiol 2006;27:13-9.
35. Rothwell PM, Warlow CP. Low risk of ischemic stroke in patients with reduced internal carotid artery lumen diameter distal to severe symptomatic carotid stenosis: cerebral protection due to low poststenotic flow? On behalf of the European Carotid Surgery Trialists' Collaborative Group. Stroke 2000;31:622-30.
36. Muller JE, Tofler GH, Stone PH. Circadian variation and triggers of onset of acute cardiovascular disease. Circulation 1989;79:733-43.
37. Moreno PR, Purushothaman KR, Fuster V, et al. Plaque neovascularization is increased in ruptured atherosclerotic lesions of human aorta: implications for plaque vulnerability. Circulation 2004;110:2032-8.
38. Narula J, Garg P, Achenbach S, et al. Arithmetic of vulnerable plaques for noninvasive imaging. Nat Clin Pract Cardiovasc Med 2008;5 Suppl 2:S2-10.
39. Lovett JK, Gallagher PJ, Rothwell PM. Reproducibility of histological assessment of carotid plaque: implications for studies of carotid imaging. Cerebrovasc Dis 2004;18:117-23.
40. Vancraeynest D, Pasquet A, Roelants V, et al. Imaging the vulnerable plaque. J Am Coll Cardiol 2011;57:1961-79.
41. Leber AW, Knez A, Becker A, et al. Accuracy of multidetector spiral computed tomography in identifying and differentiating the composition of coronary atherosclerotic plaques: a comparative study with intracoronary ultrasound. J Am Coll Cardiol 2004;43:1241-7.
42. Motoyama S, Kondo T, Sarai M, et al. Multislice computed tomographic characteristics of coronary lesions in acute coronary syndromes. J Am Coll Cardiol 2007;50:319-26.
43. ten Kate GL, van Dijk AC, van den Oord SC, et al. Usefulness of contrast-enhanced ultrasound for detection of carotid plaque ulceration in patients with symptomatic carotid atherosclerosis. Am J Cardiol 2013;112:292-8.
44. Topakian R, King A, Kwon SU, et al. Ultrasonic plaque echolucency and emboli signals predict stroke in asymptomatic carotid stenosis. Neurology 2011;77:751-8.
45. Saba L, Tamponi E, Raz E, et al. Correlation between fissured fibrous cap and contrast enhancement: preliminary results with the use of CTA and histologic validation. AJNR Am J Neuroradiol 2014;35:754-9.
46. Saba L, Raz E, Anzidei M, et al. Differences in plaque morphology and correlation of stenosis at the carotid artery bifurcation and the carotid siphon. AJR Am J Roentgenol 2013;201:1108-14.
47. Saba L, Anzidei M, Marincola BC, et al. Imaging of the carotid artery vulnerable plaque. Cardiovasc Intervent Radiol 2014;37:572-85.
48. Schroeder S, Kopp AF, Baumbach A, et al. Noninvasive detection and evaluation of atherosclerotic coronary plaques with multislice computed tomography. J Am Coll Cardiol 2001;37:1430-5.
49. de Weert TT, Ouhlous M, Zondervan PE, et al. In vitro characterization of atherosclerotic carotid plaque with multidetector computed tomography and histopathological correlation. Eur Radiol 2005;15:1906-14.
50. de Weert TT, Ouhlous M, Meijering E, et al. In vivo characterization and quantification of atherosclerotic carotid plaque components with multidetector computed tomography and histopathological correlation. Arterioscler Thromb Vasc Biol 2006;26:2366-72.
51. Saba L, Lai ML, Montisci R, et al. Association between carotid plaque enhancement shown by multidetector CT angiography and histologically validated microvessel density. Eur Radiol 2012;22:2237-45.
52. Ajduk M, Bulimbasić S, Pavić L, et al. Comparison of multidetector-row computed tomography and duplex Doppler ultrasonography in detecting atherosclerotic carotid plaques complicated with intraplaque hemorrhage. Coll Antropol 2013;37:213-9.
53. Ajduk M, Pavić L, Bulimbasić S, et al. Multidetector-row computed tomography in evaluation of atherosclerotic carotid plaques complicated with intraplaque hemorrhage. Ann Vasc Surg 2009;23:186-93.
54. Saba L, Mallarini G. Carotid plaque enhancement and symptom correlations: an evaluation by using multidetector row CT angiography. AJNR Am J Neuroradiol 2011;32:1919-25.
55. van Gils MJ, Homburg PJ, Rozie S, et al. Evolution of

atherosclerotic carotid plaque morphology: do ulcerated plaques heal? A serial multidetector CT angiography study. Cerebrovasc Dis 2011;31:263-70.
56. Hyafil F, Cornily JC, Feig JE, et al. Noninvasive detection of macrophages using a nanoparticulate contrast agent for computed tomography. Nat Med 2007;13:636-41.
57. Braunwald E. Noninvasive detection of vulnerable coronary plaques: Locking the barn door before the horse is stolen. J Am Coll Cardiol 2009;54:58-9.
58. Saba L, Argiolas GM, Siotto P, et al. Carotid artery plaque characterization using CT multienergy imaging. AJNR Am J Neuroradiol 2013;34:855-9.
59. Mannelli L, Mitsumori LM, Ferguson M, et al. Changes in measured size of atherosclerotic plaque calcifications in dual-energy CT of ex vivo carotid endarterectomy specimens: effect of monochromatic keV image reconstructions. Eur Radiol 2013;23:367-74.
60. Knauth M, von Kummer R, Jansen O, et al. Potential of CT angiography in acute ischemic stroke. AJNR Am J Neuroradiol 1997;18:1001-10.
61. Sims JR, Rordorf G, Smith EE, et al. Arterial occlusion revealed by CT angiography predicts NIH stroke score and acute outcomes after IV tPA treatment. AJNR Am J Neuroradiol 2005;26:246-51.
62. Sylaja PN, Puetz V, Dzialowski I, et al. Prognostic value of CT angiography in patients with suspected vertebrobasilar ischemia. J Neuroimaging 2008;18:46-9.
63. de Lucas EM, Sánchez E, Gutiérrez A, et al. CT protocol for acute stroke: tips and tricks for general radiologists. Radiographics 2008;28:1673-87.
64. Sharma VK, Venketasubramanian N, Teoh HL, et al. Hyperdense middle cerebral artery sign and stroke outcomes after intravenous thrombolysis. Cerebrovasc Dis 2011;31:207-8; author reply 209.
65. Riedel CH, Jensen U, Rohr A, et al. Assessment of thrombus in acute middle cerebral artery occlusion using thin-slice nonenhanced Computed Tomography reconstructions. Stroke 2010;41:1659-64.
66. Cubuk R, Tasali N, Sahin S. Hyperdense middle cerebral artery sign: an early radiological finding of acute ischaemic stroke. Emerg Med J 2011;28:344.
67. Liebeskind DS. Stroke: the currency of collateral circulation in acute ischemic stroke. Nat Rev Neurol 2009;5:645-6.
68. Rosenthal ES, Schwamm LH, Roccatagliata L, et al. Role of recanalization in acute stroke outcome: rationale for a CT angiogram-based "benefit of recanalization" model. AJNR Am J Neuroradiol 2008;29:1471-5.
69. Christoforidis GA, Mohammad Y, Kehagias D, et al. Angiographic assessment of pial collaterals as a prognostic indicator following intra-arterial thrombolysis for acute ischemic stroke. AJNR Am J Neuroradiol 2005;26:1789-97.
70. Lima FO, Furie KL, Silva GS, et al. The pattern of leptomeningeal collaterals on CT angiography is a strong predictor of long-term functional outcome in stroke patients with large vessel intracranial occlusion. Stroke 2010;41:2316-22.
71. Hill MD, Coutts SB, Pexman JH, et al. CTA source images in acute stroke. Stroke 2003;34:835-7; author reply 835-7.
72. Camargo EC, Furie KL, Singhal AB, et al. Acute brain infarct: detection and delineation with CT angiographic source images versus nonenhanced CT scans. Radiology 2007;244:541-8.
73. Chen HM, Chen CC, Tsai FY, et al. Cerebral sinovenous thrombosis. Neuroimaging diagnosis and clinical management. Interv Neuroradiol 2008;14 Suppl 2:35-40.
74. Tsai FY, Wang AM, Matovich VB, et al. MR staging of acute dural sinus thrombosis: correlation with venous pressure measurements and implications for treatment and prognosis. AJNR Am J Neuroradiol 1995;16:1021-9.
75. Shroff M, deVeber G. Sinovenous thrombosis in children. Neuroimaging Clin N Am 2003;13:115-38.
76. Kriss VM. Hyperdense posterior falx in the neonate. Pediatr Radiol 1998;28:817-9.
77. Pappadà G, Cesana C, Pirovano M, et al. Venous outflow as a criterion of impairment of cerebral vascular reserve. J Neurosurg Sci 2009;53:101-5.
78. Liebeskind DS. Collateral circulation. Stroke 2003;34:2279-84.
79. Wintermark M, Meuli R, Browaeys P, et al. Comparison of CT perfusion and angiography and MRI in selecting stroke patients for acute treatment. Neurology 2007;68:694-7.
80. Hopyan J, Ciarallo A, Dowlatshahi D, et al. Certainty of stroke diagnosis: incremental benefit with CT perfusion over noncontrast CT and CT angiography. Radiology 2010;255:142-53.
81. Allmendinger AM, Tang ER, Lui YW, et al. Imaging of stroke: Part 1, Perfusion CT--overview of imaging technique, interpretation pearls, and common pitfalls. AJR Am J Roentgenol 2012;198:52-62.
82. Koenig M, Klotz E, Luka B, et al. Perfusion CT of the brain: diagnostic approach for early detection of ischemic stroke. Radiology 1998;209:85-93.
83. Nabavi DG, Cenic A, Craen RA, et al. CT assessment of cerebral perfusion: experimental validation and initial

clinical experience. Radiology 1999;213:141-9.
84. Saba L, Anzidei M, Piga M, et al. Multi-modal CT scanning in the evaluation of cerebrovascular disease patients. Asvide 2014;241.
85. Wintermark M, Maeder P, Thiran JP, et al. Quantitative assessment of regional cerebral blood flows by perfusion CT studies at low injection rates: a critical review of the underlying theoretical models. Eur Radiol 2001;11:1220-30.
86. Konstas AA, Goldmakher GV, Lee TY, et al. Theoretic basis and technical implementations of CT perfusion in acute ischemic stroke, part 1: Theoretic basis. AJNR Am J Neuroradiol 2009;30:662-8.
87. Powers WJ, Grubb RL Jr, Raichle ME. Physiological responses to focal cerebral ischemia in humans. Ann Neurol 1984;16:546-52.
88. Hacke W, Albers G, Al-Rawi Y, et al. The Desmoteplase in Acute Ischemic Stroke Trial (DIAS): a phase II MRI-based 9-hour window acute stroke thrombolysis trial with intravenous desmoteplase. Stroke 2005;36:66-73.
89. Marchal G, Young AR, Baron JC. Early postischemic hyperperfusion: pathophysiologic insights from positron emission tomography. J Cereb Blood Flow Metab 1999;19:467-82.
90. Nguyen TB, Lum C, Eastwood JD, et al. Hyperperfusion on perfusion computed tomography following revascularization for acute stroke. Acta Radiol 2005;46:610-5.
91. Lui YW, Tang ER, Allmendinger AM, et al. Evaluation of CT perfusion in the setting of cerebral ischemia: patterns and pitfalls. AJNR Am J Neuroradiol 2010;31:1552-63.
92. Coutts SB, Modi J, Patel SK, et al. CT/CT angiography and MRI findings predict recurrent stroke after transient ischemic attack and minor stroke: results of the prospective CATCH study. Stroke 2012;43:1013-7.
93. Coutts SB, Modi J, Patel SK, et al. What causes disability after transient ischemic attack and minor stroke?: Results from the CT and MRI in the Triage of TIA and minor Cerebrovascular Events to Identify High Risk Patients (CATCH) Study. Stroke 2012;43:3018-22.
94. Demchuk AM, Dowlatshahi D, Rodriguez-Luna D, et al. Prediction of haematoma growth and outcome in patients with intracerebral haemorrhage using the CT-angiography spot sign (PREDICT): a prospective observational study. Lancet Neurol 2012;11:307-14.
95. Parsons M, Spratt N, Bivard A, et al. A randomized trial of tenecteplase versus alteplase for acute ischemic stroke. N Engl J Med 2012;366:1099-107.
96. Brenner DJ, Hall EJ. Computed tomography--an increasing source of radiation exposure. N Engl J Med 2007;357:2277-84.
97. Dani KA, Muir KW. Do iodinated contrast agents impair fibrinolysis in acute stroke? A systematic review. AJNR Am J Neuroradiol 2010;31:170-4.
98. Macdougall NJ, McVerry F, Baird S, et al. Iodinated contrast media and cerebral hemorrhage after intravenous thrombolysis. Stroke 2011;42:2170-4.
99. http://www.fda.gov/MedicalDevices/Safety/AlertsandNotices/ucm193293.htm
100. Allmendinger AM, Tang ER, Lui YW, et al. Imaging of stroke: Part 1, Perfusion CT--overview of imaging technique, interpretation pearls, and common pitfalls. AJR Am J Roentgenol 2012;198:52-62.
101. McCollough CH, Primak AN, Braun N, et al. Strategies for reducing radiation dose in CT. Radiol Clin North Am 2009;47:27-40.
102. Smith AB, Dillon WP, Gould R, et al. Radiation dose-reduction strategies for neuroradiology CT protocols. AJNR Am J Neuroradiol 2007;28:1628-32.

Cite this article as: Saba L, Anzidei M, Piga M, Ciolina F, Mannelli L, Catalano C, Suri JS, Raz E. Multi-modal CT scanning in the evaluation of cerebrovascular disease patients. Cardiovasc Diagn Ther 2014;4(3):245-262. doi: 10.3978/j.issn.2223-3652.2014.06.05

